A Strategy of Direct Power Control for PWM Rectifier Reducing Ripple in Instantaneous Power

T. Mohammed Chikouche, K. Hartani

Abstract—In order to solve the instantaneous power ripple and achieve better performance of direct power control (DPC) for a three-phase PWM rectifier, a control method is proposed in this paper. This control method is applied to overcome the instantaneous power ripple, to eliminate line current harmonics and therefore reduce the total harmonic distortion and to improve the power factor. A switching table is based on the analysis on the change of instantaneous active and reactive power, to select the optimum switching state of the three-phase PWM rectifier. The simulation result shows feasibility of this control method.

Keywords—Power quality, direct power control, power ripple, switching table, unity power factor.

I. INTRODUCTION

IN recent years, three-phase PWM rectifiers have been widely applied in many variety of industrial applications dues its advantages, such as absorption of sinusoidal current with low harmonic distortion and the possibility of operation with a power factor unity, good DC-bus voltage regulation ability and bidirectional power flow [1]-[3].

Various control strategies are proposed in [4]-[6] which are classified into two categories: (1) Voltage Oriented Control (VOC) similar to the vector control of electrical machines [7]-[9], and (2) DPC similar to the direct torque control of electrical machines [10]. These strategies reach the same goals, such as the unity power factor and the sinusoidal input current waveform, but their principles are different. This method has some disadvantages such as coupling which occurs between the active and reactive components and the problem of coordinate transformation. However, the DPC controls the active and reactive power directly. Compared to VOC, the DPC can achieve very quick response with simple structure by selecting a voltage vector from predefined switching table. The latter is not accurate for it gives large power ripples [11], [12].

The main advantages of DPC are absence of coordinate transformation, no internal current control loop and no PWM modulator block. In the conventional DPC [13], the active and reactive power are estimated using grid voltage and current measurements based on instantaneous power theory [14]. The hysteresis band control technique is used to compare instantaneous errors of active and reactive power. The output of the two hysteresis controller and the position of the voltage vector constitute the inputs of the switching table which imposes the switching state of the PWM rectifier [15], [16].

The disadvantages of conventional DPC are high active power ripple and slow transient response to the step changes in power load. The switching table has a very important role in the performance of the DPC [17]. However, the use of only one voltage vector in the conventional switching table during one control period leads to high power ripples. The conventional switching table illustrated in [18], demonstrates that it is not satisfactory in the controlling of the active and reactive power.

The main aim of this paper is to propose a switching method for DPC to improve DC-bus voltage regulation by directly controlling the instantaneous active and reactive power, eliminate the harmonic current and achieve a unity power factor operation.

This paper is arranged as follows: A model of a three-phase rectifier is presented in section two. A principle of the proposed DPC with a switching table is carried out based on the analysis of the instantaneous active and reactive power, including steady state performance, dynamic response and robustness against external load disturbance. Simulations by using MATLAB/Simulink are performed to study the characteristics and performance of the proposed method under steady state and transient conditions. To conclude, there is a thorough conclusion.

II. MODEL OF THREE-PHASE PWM RECTIFIER

The topology of three-phase bidirectional voltage-source PWM rectifier (VSR) is shown in Fig. 1. The VSR is connected to the three-phase AC source via smoothing L and internal resistance R. The inductance acts as a line filter for smoothing the line currents with the minimum ripples. Insulated Gate Bipolar Transistor (IGBTs) are used as the VSR power switches since IGBTs have features of high frequency switching applications. The DC-link capacitor C, is used for filtering the ac components so that DC voltage with minimum ripple can be achieved at the output of VSR. It is assumed that a pure resistive load R_L is connected at the DC-link capacitor C [19].

The model of the PWM rectifier can be expressed in (a,b,c) frame as:

$$\begin{bmatrix} v_a \\ v_b \\ v_c \end{bmatrix} = R \begin{bmatrix} i_a \\ i_b \\ i_c \end{bmatrix} + L \frac{d}{dt} \begin{bmatrix} i_a \\ i_b \\ i_c \end{bmatrix} + \begin{bmatrix} v_{ra} \\ v_{rb} \\ v_{rc} \end{bmatrix} \qquad (1)$$

T. Mohammed Chikouche is with the Electrotechnical Engineering Laboratory, University Tahar Moulay of Saida, Algeria (e-mail: tchikouche@yahoo.fr).
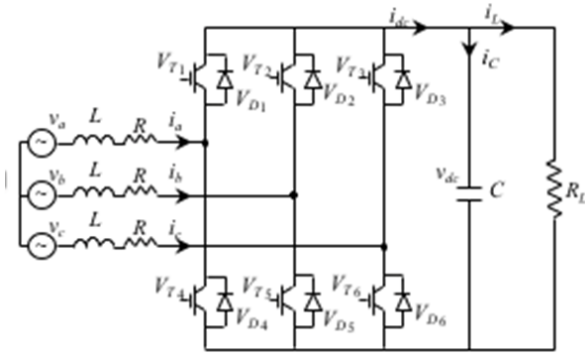K. Hartani is with the Electrotechnical Engineering Laboratory, University Tahar Moulay of Saida, Algeria.

Fig. 1 Topology of three-phase PWM rectifier

$$c\frac{dv_{dc}}{dt} = S_a i_a + S_b i_b + S_c i_c \quad (2)$$

The phase voltage at the poles of the converter is equal to:

$$\begin{bmatrix} v_{ra} \\ v_{rb} \\ v_{rc} \end{bmatrix} = \frac{v_{dc}}{3} \begin{bmatrix} 2 & -1 & -1 \\ -1 & 2 & -1 \\ -1 & -1 & 2 \end{bmatrix} \begin{bmatrix} S_a \\ S_b \\ S_c \end{bmatrix} \quad (3)$$

The instantaneous apparent power can be expressed in several different manners as (4):

$$S = v\bar{i} = p + jq = v_a i_a + v_b i_b + v_c i_c +$$
$$j\frac{1}{\sqrt{3}}\left[(v_b - v_c)i_a + (v_c - v_a)i_b + (v_a - v_b)i_c\right] \quad (4)$$

where $\bar{i}$ is the complex conjugate of line current i; j is the imaginary unit.

The instantaneous active power and reactive power at the grid side can be calculated from grid voltage and current as [20], [22]:

$$\begin{cases} p = v_a i_a + v_b i_b + v_c i_c \\ q = \frac{1}{\sqrt{3}}\left[(v_b - v_c)i_a + (v_c - v_a)i_b + (v_a - v_b)i_c\right] \end{cases} \quad (5)$$

From the power model of PWM rectifier, we can know that different switching states have different influences on the active and reactive power. It is possible to select optimal switching states to adjust active and reactive power.

III. Switching Table for DPC

A. Principle of the DPC

The DPC technique is based on the direct control of active and reactive power of PWM rectifier. The instantaneous values of active p and reactive q power are estimated by (4).

The active power reference is obtained from the voltage controller of the DC bus. However, the reactive power reference is set to zero to get unity power factor.

As shown in Fig. 2, the output of the two hysteresis controllers constitutes the inputs of the proposed switching table which selects the optimal switching states of PWM rectifier [10]-[14].

The digitized signals S_p, S_q which are provided by a fix band hysteresis comparator can show whether should increase or reduce (decrease) the active or reactive power.
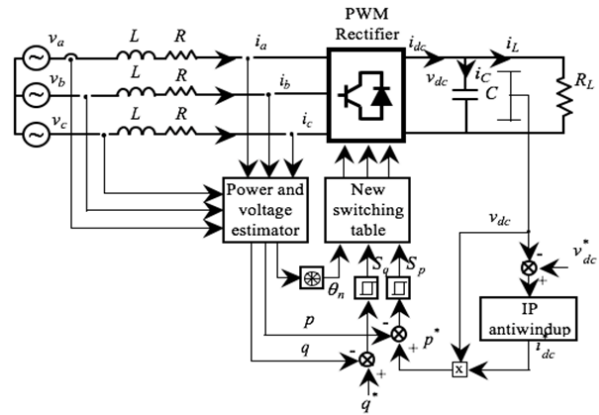

Fig. 2 Proposed DPC configuration of three-phase PWM rectifier

The power model of PWM rectifier is given as [21]:

$$\begin{cases} L\frac{dp}{dt} = -R_p - \omega L_q - (v_a v_{ra} + v_\beta v_{r\beta}) + (v_\alpha^2 + v_\beta^2) \\ L\frac{dq}{dt} = -R_q + \omega L_p - (v_a v_{ra} - v_\beta v_{r\beta}) \end{cases} \quad (6)$$

From the power model of PWM rectifier, we can know that different switching states have different influences on the active and reactive power. It is possible to select the proper switching states to adjust the active and reactive power. The phase of the power-source voltage vector is converted to the digitized signal θ_n. For this purpose, the stationary coordinates are divided into 12 sectors, as shown in Fig. 3, and the sectors can be numerically expressed as:

$$(n-2)\frac{\pi}{6} \leq \theta_n \leq (n-1)\frac{\pi}{6} \qquad n = 1, 2, ..., 12 \quad (7)$$

B. Vector Selection in the Switching Table

The switching table is formed from the output of the two hysteresis controllers (S_p, S_q) and the angular position θ_n of the voltage vector. $S_P = 1$ stands for the need to increase the active power, while $S_P = 0$ denotes the need to decrease the active power. So, it is the case of the S_q.
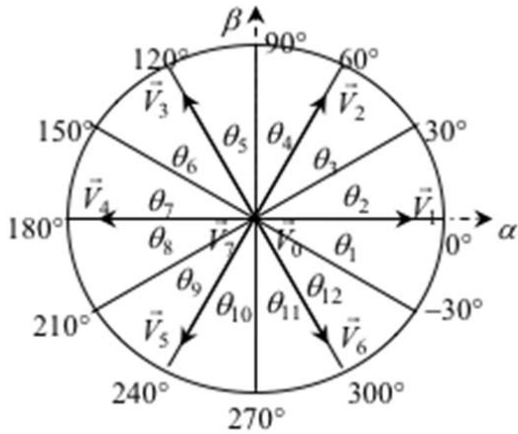
Fig. 3 12 sectors in stationary coordinates, to specify power-source voltage vector position and rectifier voltage vectors

$$\begin{cases} \dfrac{dp}{dt} = \dfrac{3}{2}\dfrac{V_M^2}{L} - \dfrac{V_M v_{dc}}{L} \cos\left[\omega t - \dfrac{\pi}{3}(k-1)\right] \\ \dfrac{dq}{dt} = -\dfrac{V_M v_{dc}}{L} \sin\left[\omega t - \dfrac{\pi}{3}(k-1)\right] + \omega p \end{cases} \quad (8)$$

where $k = 1,2,3,4,5,6$, corresponding to the no zero selected voltage vector number shown in Fig. 3.

The variation of active power and reactive power versus grid voltage position for various rectifier voltage vectors are depicted in Fig. 4.

In order to achieve better performance of system, the switching table should be synthesized based on the variation of active and reactive power for various rectifier voltage vectors in each sector, as shown in Fig. 4. Take the first three sectors for example, the signs of slope in active and reactive power are illustrated in Table I [22].

According to the inputs S_P and S_q, together with the sector information, the proper rectifier input voltage vector can be chosen and the corresponding switching stable will be sent to trigger the IGBTs of the main circuit.

Considering the value of R is small enough to be neglected, the instantaneous active and reactive power can be rewritten as:

TABLE I
SIGNS OF SLOPE IN ACTIVE AND REACTIVE POWER FOR FIRST THREE SECTOR

Sector	dp/dt		dq/dt	
	$\rangle 0 (S_p = 1)$	$\langle 0 (S_p = 0)$	$\rangle 0 (S_q = 1)$	$\langle 0 (S_q = 0)$
θ_1	V_2, V_3, V_4, V_5	V_1, V_6	V_1, V_2, V_3	V_4, V_5, V_6
θ_2	V_3, V_4, V_5, V_6	V_1, V_2	V_2, V_3, V_4	V_1, V_5, V_6
θ_3	V_3, V_4, V_5, V_6	V_1, V_2	V_2, V_3, V_4	V_1, V_5, V_6

The switching table for DPC of PWM rectifier can be summarized in Table II.

TABLE II
THE SWITCHING TABLE FOR DPC OF PWM RECTIFIER

S_P	S_q	θ_1	θ_2	θ_3	θ_4	θ_5	θ_6	θ_7	θ_8	θ_9	θ_{10}	θ_{11}	θ_{12}
1	0	V_4	V_5	V_5	V_6	V_6	V_1	V_1	V_2	V_2	V_3	V_3	V_4
	1	V_3	V_4	V_4	V_5	V_5	V_6	V_6	V_1	V_1	V_2	V_2	V_3
0	0	V_6	V_1	V_1	V_2	V_2	V_3	V_3	V_4	V_4	V_5	V_5	V_6
	1	V_1	V_2	V_2	V_3	V_3	V_4	V_4	V_5	V_5	V_6	V_6	V_1
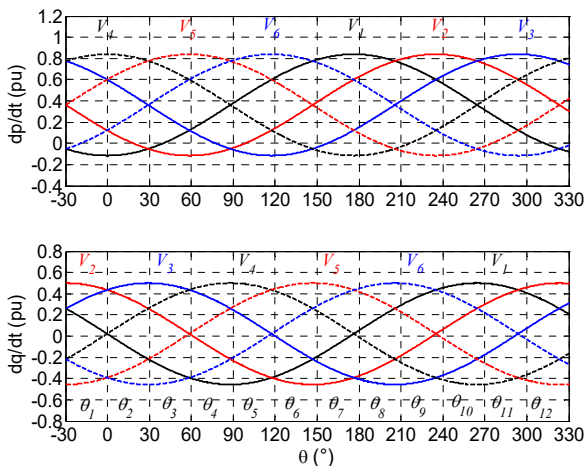
C. Control of the DC-Link Voltage

The basic operation principle of VSR is to regulate the DC-link voltage v_{dc} at load, at a reference value v_{dc}^*, while maintaining a desired grid side power factor. The value of v_{dc}^* has to be high enough to keep the diodes of converter blocked and maintain the controller stability.

Generally, the minimum DC-link voltage can be determined by the peak value of line-to-line grid, i.e.

$$V_{dc} \succ \sqrt{3}\sqrt{2}V_{(RMS)} = 2.45 V_{(RMS)}$$

The error between rectified voltage v_{dc} and reference v_{dc}^* is then fed to the anti-windup IP controller to obtain the current component command i_{dc}^* [19]. The product of rectifier voltage v_{dc} and the current reference obtained at the output of the anti-windup IP controller gives the active power reference.

Fig. 4 Variation of active and reactive power for various rectifier voltage vectors

TABLE III
P ANTI-WINDUP ALGORITHM

Err=Vdc_ref-Vdc;
Tintegral(n+1)=Tintegral(n)+ki*T*Err;
idc_ref=kp*(Tintegral(n+1)- Vdc);

if abs(idc_ref)>=abs(idc_max)
  idc_ref =sign(idc_ref)*idc_max;
  Tintegral(n+1)=idc_ref /kp+ Vdc;
End;

IV. RESULTS AND DISCUSSION

To evaluate the performance of the proposed DPC with switching table, the simulation test is carried out on a two-level three-phase PWM rectifier. In this simulation test, we have introduced some changes the reference of the DC bus voltage (between $t = 0.30s$ and $t = 0.70s$), and then introduced a perturbation characterized by a load resistance increasing between the instant $t = 0.45s$ and $t = 0.55s$. The main parameters of the simulation circuit are given in Table IV.

TABLE IV
RECTIFIER PARAMETERS

|	
The input phase voltage:	$V = 125V$ / $f = 50Hz$
The input inductance:	$L = 37mH$
The input resistance:	$R = 0,3\Omega$
The output capacitor:	$C_{dc} = 1100\mu F$
The output voltage:	$V_{dc} = 350V$

Fig. 5 (a) shows simulation waveform that the load increases from 500Ω to 750Ω at $0.45s$ and at $0.55s$. We notice from Fig. 5 (b) that the response of the DC-bus voltage v_{dc} follows perfectly its reference. There is a satisfactory steady state operation with no static error, which shows that the proposed analytical approach for the design of the IP regulator is fairly rigorous, Fig. 5 (c). The application of the disturbance affects the DC bus voltage with a weak drop of the order of 0.3% for a brief period of 0.05 s, Fig. 5 (c). This signifies that the voltage IP regulator acts well on the rejection of this disturbance. To show the efficiency of the IP regulator, the normalized error of the DC bus voltage is shown in Fig. 5 (d).

The introduction of the perturbation characterized by an increase in the load resistance applied at the instant $t = 0.45s$ in steady state causes a decrease in the load current which responds instantaneously to this variation and after the instant $t = 0.55s$, the current i_L is kept constant at its nominal value 0.9A, Fig. 5 (e).

The current response is practically instantaneous, as shown in Fig. 6 (a), which represents the three currents at the input of the rectifier corresponding to the current operation. In transient mode, these currents show a transient with a rapid increase when the load is applied. Then, they stabilize at an amplitude of 1.55A after the instant $t = 0.55s$, Fig. 6 (b). We notice that these grid currents are sinusoidal which gives a low rate of harmonic distortion. Fig. 6 (c) shows the harmonic
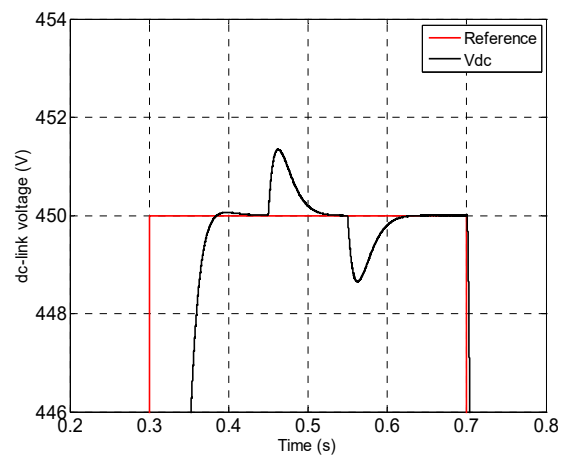
spectrum of the response of the grid current i_a. It is noted that all the low render harmonics are well attenuated, which gives a rate of harmonic distortion (THD =0.96%).
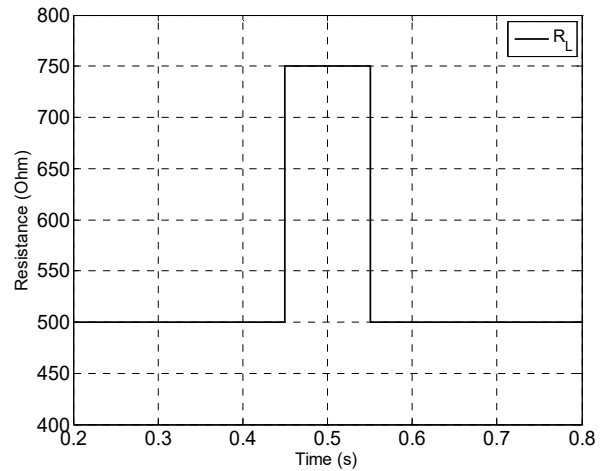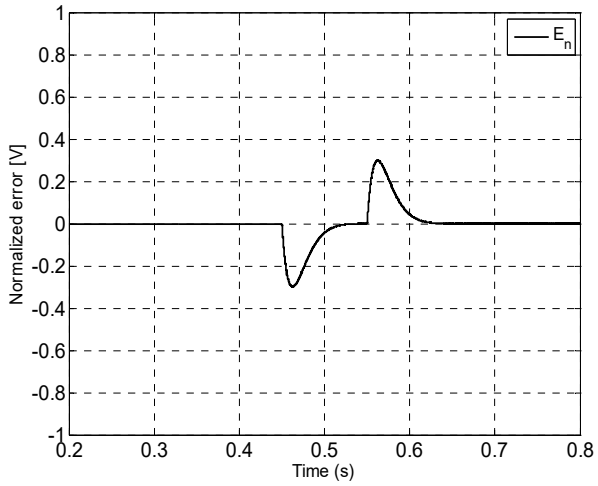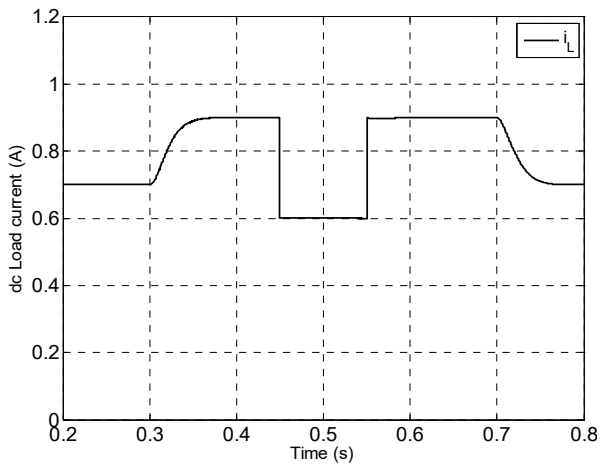

(a) Load charge
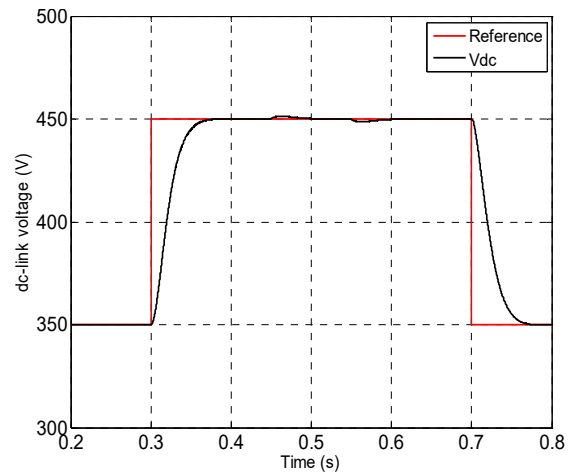
(b) DC output voltage

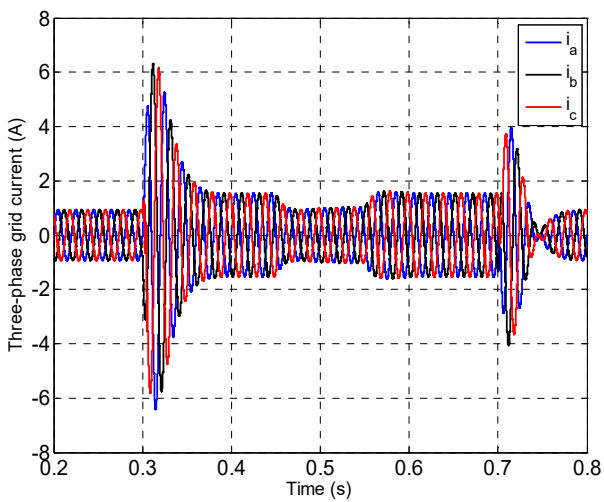(c) Zoom of the DC output voltage

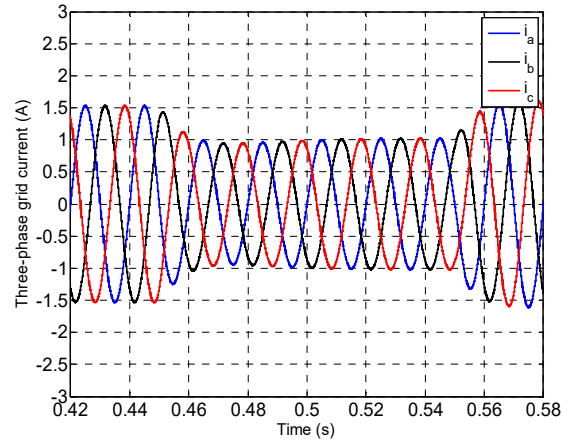(d) Normalized error of the DC output voltage

(e) Load current

Fig. 5 Simulation result of the PWM rectifier with under load disturbance (50% variation of resistance at 0.45s and 0.55s)

(a) Line current

(b) Zoom of line current

(c) Line current spectrum of phase a

Fig. 6 The waveforms of three phase grid current and line current spectrum
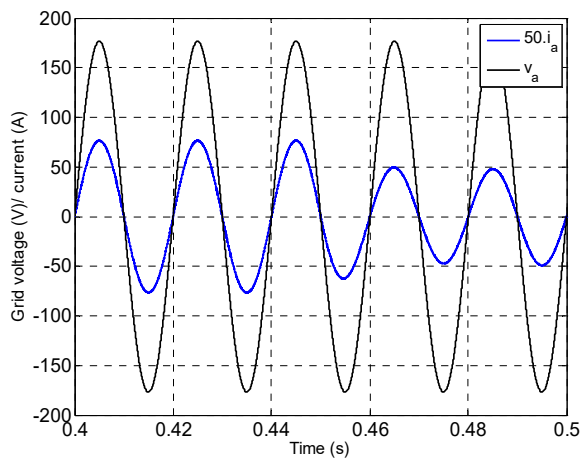

Fig. 7 Voltage and current waveforms of phase a

Fig. 7 shows that the grid current i_a is phase with the grid voltage, which gives a unit power factor.

The power response is illustrated in Fig. 8. The active power increases from 245 W to 406 W at $t = 0.4s$, and then decreases to 270 W between $t = 0.45s$ and $t = 0.55s$, and then increases to 406 W. After $t = 0.37s$, it stabilizes at the initial value (245 W).

The proposed DPC with a switching table adjusts well the active power in all sectors when the load power decreases. It is clearly seen that in Fig. 8, the reactive power is kept at zero to achieve a unit power factor. It can be seen that the proposed DPC achieves a decoupled control of active and reactive power. It can be seen that the proposed DPC achieves a decoupled control of active and reactive power. The simulation results prove that the proposed DPC is much better when the load changes.
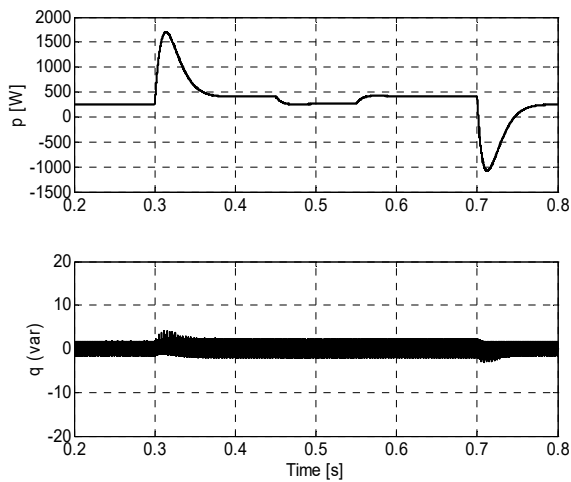

Fig. 8 Voltage and current waveforms of phase a

V. CONCLUSION

This paper introduces a control method for DPC of three-phase PWM rectifier based on the analysis of instantaneous active and reactive power. The proposed method can choose a more appropriate switching state. Hence, it can eliminate line current harmonics, reduce the total harmonic distortion, achieve unity power factor, and keep the instantaneous active and reactive power and DC-bus voltage at their desired values. Simulation results show a good performance of proposed method and provide a good regulation of output DC voltage and give better performances in steady state and dynamic response disturbance rejection.

REFERENCES

[1] O. Aissa, S. Moulahoum, N. Kabache, and H. Houassine, "Improved power quality PWM rectifier based on fuzzy logic direct power controller," in Harmonics and Quality of Power (ICHQP), 2014 IEEE 16th International Conference on, 2014, pp. 219-223.
[2] M. U. Hashmi, "Design and Development of UPF Rectifier in a Microgrid Environment," Indian Institute of Technology Bombay, 2012.
[3] J. R. Rodríguez, J. W. Dixon, J. R. Espinoza, J. Pontt, and P. Lezana, "PWM regenerative rectifiers: State of the art," IEEE Transactions on Industrial Electronics, vol. 52, pp. 5-22, 2005.
[4] J. Huang, A. Zhang, H. Zhang, and J. Wang, "A novel fuzzy-based and voltage-oriented direct power control strategy for rectifier," in IECon 2011-37th Annual Conference on IEEE Industrial Electronics Society, 2011, pp. 1115-1119.
[5] J P. Liutanakul, S. Pierfederici, and F. Meibody-Tabar, "Application of SMC with I/O feedback linearization to the control of the cascade controlled-rectifier/inverter-motor drive system with small dc-link capacitor," IEEE Transactions on Power Electronics, vol. 23, pp. 2489-2499, 2008.
[6] J. Norniella, J. Cano, G. Orcajo, C. Rojas, J. Pedrayes, M. Cabanas, et al., "Optimization of direct power control of three-phase active rectifiers by using multiple switching tables," in International Conference of Renewable Energies and Power Quality (ICREPQ'10), 2010.
[7] P. Ambade, S. Premakumar, R. Patel, H. Chaudhari, A. Tillu, U. Yerge, et al., "Direct power control PWM rectifier using switching table for series resonant converter capacitor charging pulsed power supply," in Recent Trends in Electronics, Information & Communication Technology (RTEICT), IEEE International Conference on, 2016, pp. 758-762.
[8] M. Malinowski, M. P. Kazmierkowski, and A. M. Trzynadlowski, "A comparative study of control techniques for PWM rectifiers in AC adjustable speed drives," IEEE Transactions on power electronics, vol. 18, pp. 1390-1396, 2003.
[9] M. Razali, M. Rahman, and N. A. Rahim, "Real-time implementation of dq control for grid connected three phase voltage source converter," in Industrial Electronics Society, IECON 2014-40th Annual Conference of the IEEE, 2014, pp. 1733-1739.
[10] Fekik, H. Denoun, N. Benamrouche, N. Benyahia, A. Badji, and M. Zaouia, "Comparative analysis of direct power control and direct power control with space vector modulation of PWM rectifier," in Control Engineering & Information Technology (CEIT), 2016 4th International Conference on, 2016, pp. 1-6.
[11] Y. Zhang, Y. Peng, and H. Yang, "Performance improvement of two-vectors-based model predictive control of PWM rectifier," IEEE Transactions on Power Electronics, vol. 31, pp. 6016-6030, 2016.
[12] Y. Zhang, C. Qu, Z. Li, and Y. Zhang, "Mechanism analysis and experimental study of table-based direct power control," in Electrical Machines and Systems (ICEMS), 2013 International Conference on, 2013, pp. 2213-2218.
[13] T. Ohnishi, "Three phase PWM converter/inverter by means of instantaneous active and reactive power control," in Industrial Electronics, Control and Instrumentation, 1991. Proceedings. IECON'91, 1991 International Conference on, 1991, pp. 819-824.
[14] M. Razali and M. Rahman, "Performance analysis of three-phase PWM rectifier using direct power control," in Electric Machines & Drives Conference (IEMDC), 2011 IEEE International, 2011, pp. 1603-1608.
[15] Bouafia, F. Krim, and J.-P. Gaubert, "Direct power control of three-phase PWM rectifier based on fuzzy logic controller," in Industrial Electronics, 2008. ISIE 2008. IEEE International Symposium on, 2008, pp. 323-328.
[16] J. Lamterkati, M. Khaffalah, and L. Ouboubker, "Fuzzy logic based impoved direct power control of three-phase PWM rectifier," in Electrical and Information Technologies (ICEIT), 2016 International Conference on, 2016, pp. 125-130.
[17] Baktash, A. Vahedi, and M. Masoum, "Improved switching table for direct power control of three-phase PWM rectifier," in Power Engineering Conference, 2007. AUPEC 2007. Australasian Universities, 2007, pp. 1-5.
[18] T. Noguchi, H. Tomiki, S. Kondo, and I. Takahashi, "Direct power control of PWM converter without power-source voltage sensors," IEEE Transactions on Industry Applications, vol. 34, pp. 473-479, 1998.
[19] K. Hartani and Y. Miloud, "Control strategy for three phase voltage source PWM rectifier based on the space vector modulation," Advances in Electrical and Computer Engineering, vol. 10, pp. 61-65, 2010.
[20] L. Dalessandro, S. D. Round, and J. W. Kolar, "Center-point voltage balancing of hysteresis current controlled three-level PWM rectifiers," IEEE Transactions on Power Electronics, vol. 23, pp. 2477-2488, 2008.
[21] H. Zhou, X. Zha, Y. Jiang, and W. Hu, "A novel switching table for direct power control of three-phase PWM rectifier," in Power Electronics and Application Conference and Exposition (PEAC), 2014 International, 2014, pp. 858-863.
[22] Gong, K. Wang, J. Zhang, J. You, Y. Luo, and Z. Wenyi, "Advanced switching table for direct power control of a three-phase PWM rectifier," in Transportation Electrification Asia-Pacific (ITEC Asia-Pacific), 2014 IEEE Conference and Expo, 2014, pp. 1-5.